Performance of a dual anode nickel–hydrogen cell

Randall F. Gahn
NASA Lewis Research Center, Cleveland, OH 44135 (U.S.A.)

Abstract

An experimental study was conducted to characterize the voltage performance of a nickel–hydrogen cell containing a hydrogen electrode on both sides of the nickel electrode. The dual anode cell was compared with a conventional single anode cell using the same nickel electrode. Higher discharge voltages and lower charge voltages were obtained with the dual anode cell during constant current discharges to 10*C*, pulse discharges to 8*C* and polarization measurements at 50% state-of-charge.

Introduction

Nickel–hydrogen batteries are currently being used in numerous geosynchronous orbit (GEO) applications and also on the Hubble Space Telescope in low-earth orbit (LEO) [1]. GEO applications require approximately 100 charge/discharge cycles per year whereas LEO applications require about 6000 cycles per year. Recent improvements in the cycle life indicate nickel–hydrogen batteries could meet the five-year life requirements for a LEO satellite (e.g. Space Station Freedom) and replace nickel–cadmium batteries for other LEO applications [2, 3]. Reduction in battery weight to increase the specific energy is also being addressed through the development of lighter weight nickel electrodes [4].

This investigation focused on the improvement in the voltage performance of the nickel–hydrogen cell by reducing the polarization factors of the components. Voltage losses in a cell are a function of the ohmic resistance of the components and the electrochemical polarization parameters of the electrodes [5]. The ohmic resistance fraction of the total polarization is determined by the separator conductivity, the electrolyte concentration, the compression of the components and the resistivity of the electrode current collectors. The electrochemical polarization of the total polarization is attributed to the kinetics of the reactions and mass transport of the ionic species. Reduction in the effect of any of these variables will improve the voltage performance of the cell.

In an attempt to reduce cell voltage losses a second hydrogen electrode was introduced into the cell on the other side of the nickel electrode. (A second separator was also added between the second hydrogen electrode and the nickel electrode.) The addition of the second anode reduces the current density on the hydrogen electrode by one-half and the additional

0378-7753/91/$3.50

separator provides electrolyte on the 'backside' of the nickel electrodes and in effect shortens the electrolyte diffusion path into the nickel electrode by one-half. Thus, these modification should reduce the overall polarization losses by about one-half.

The purpose of this investigation was to experimentally evaluate the voltage characteristics of a nickel–hydrogen cell containing a dual anode. The performance was compared to that of a cell using a single anode and the same nickel electrode. (The evaluation of the same nickel electrode eliminates any differences in nickel electrode characteristics.)

A second objective of this study was to evaluate the dual anode cell design using thick nickel electrodes for potential pulse power applications. However, only the analysis of a standard thickness (30 mil/0.76 mm) electrode has been completed and is reported herein.

Experimental

Sketches of a conventional nickel–hydrogen cell and the dual anode cell used in this experiment are shown in Fig. 1. The dual anode sketch shows the additional hydrogen electrode and separator placed on top of the nickel electrode. Cell components were 3.5 in. (8.9 cm) diameter pineapple-slice design. The nickel electrode was obtained from the Hughes Aircraft Company. The hydrogen electrodes were obtained from Eagle-Picher Industries. The same nickel electrode was used in both cells. A layered-type separator was used with each design and consisted of one layer of Zircar cloth next to the hydrogen electrode and a layer of radiation-grafted polyethylene film next to the nickel electrode. Voltage leads were spot-welded to the base of each electrode. Following assembly the cells were vacuum filled with 26% potassium hydroxide electrolyte and installed in a boilerplate pressure vessel. The current leads and voltage sensing leads were fed through a Conax fitting

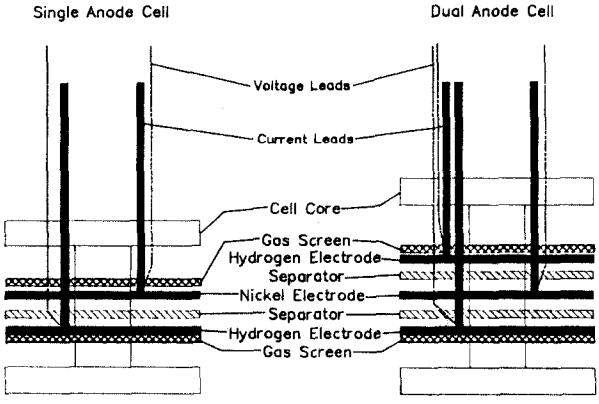

Fig. 1. Schematic diagrams of the single anode and dual anode cells. Electrode area = 50.0 cm^2.

mounted in the lid. The vessel was evacuated and then pressurized with 150 psi of hydrogen.

Performance of each cell design was determined with constant current discharges from $C/4$ to $10C$, constant current charges at $C/2$, pulse discharges at $2C$, $4C$ and $8C$ and voltage–current relationships for 15 s charges and discharges at 50% depth-of-discharge (DOD).

Results and discussion

The ampere hour (A h) capacity of each cell design was determined by discharging the cell at the $C/4$ rate to 0.1 V. Capacities measured for the single anode cell and the dual anode cell were 1.25 and 1.27 A h, respectively. For both designs, however, performance of the cell was based on a capacity of 1.3 A h. Charging for all cycles was done at the $C/2$ rate with a 5% to 10% overcharge. Following all discharges the cell was returned to the same reference point by discharging at the $C/4$ rate to 0.1 V before starting the next cycle.

Discharge performance at constant current as a function of cell capacity was measured at $C/4$, $C/2$, C, $2C$, $4C$, $6C$, $8C$ and $10C$ for both cell designs. Voltage profile for the single anode cell is shown in Fig. 2 and for the dual anode cell in Fig. 3. As expected, the discharge A h capacity decreased as the current increased, but both cell designs were similar over the entire range. At the $10C$ rate the capacity to 0.1 V was 1.09 A h for both cells. (Note that the cell voltage was measured at the base of the electrodes and does not reflect voltage losses associated with the current leads and connections when the measurement is taken outside the pressure vessel.)

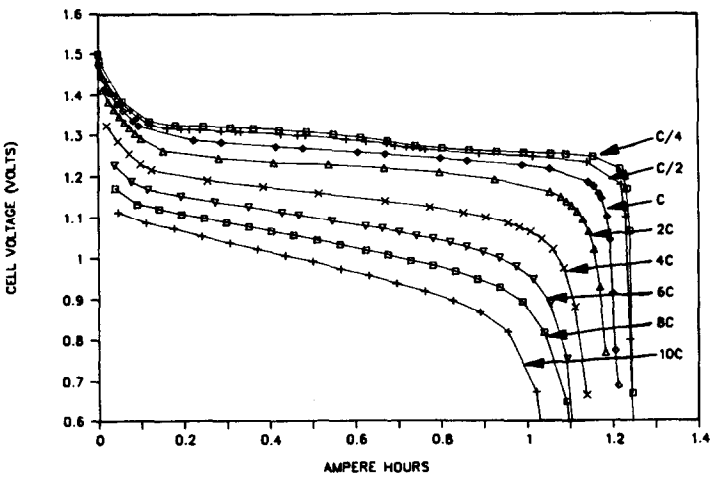

Fig. 2. Constant current discharge voltage profile of the conventional single anode nickel–hydrogen cell. Voltage measured at base of electrodes. $C = 1.3$.

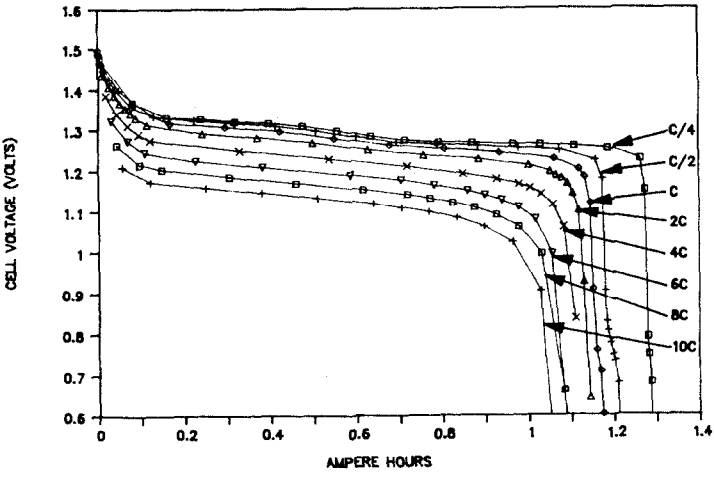

Fig. 3. Constant current discharge voltage profile of the dual anode nickel–hydrogen cell. Voltage measured at base of electrodes. $C = 1.3$.

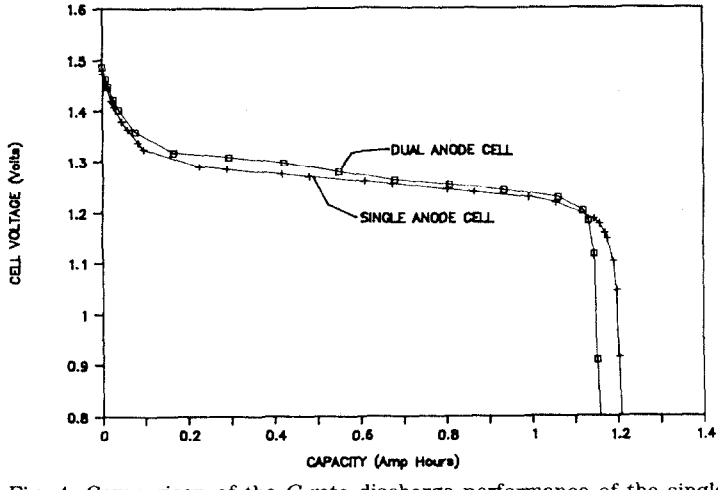

Fig. 4. Comparison of the C rate discharge performance of the single anode and dual anode cells. $C = 1.3$.

Comparison of constant current discharges for the two designs at the C and $10C$ rates are shown in Figs. 4 and 5. At both rates the voltage of the dual anode cell is higher than the conventional single anode cell. The discharge capacities at the C rate were similar (about 1.2 A h) for both designs. The $10C$ discharge capacities were also unaffected by the cell design. The voltage difference between the C rate discharge curves over the entire discharge is 10–20 mV, but at the $10C$ rate the voltage difference increased with the depth-of-discharge. Figures 6 and 7 show the difference in the constant current discharge voltages between the two cells at the mid-point

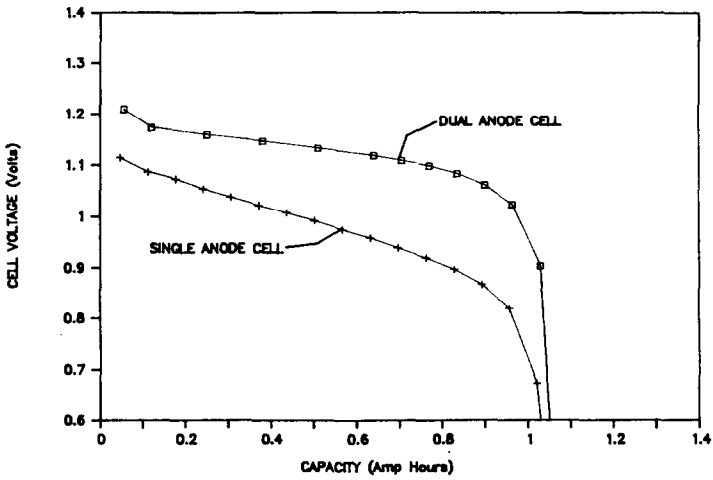

Fig. 5. Comparison of the 10C discharge performance of the single anode and dual anode cells. $C = 1.3$.

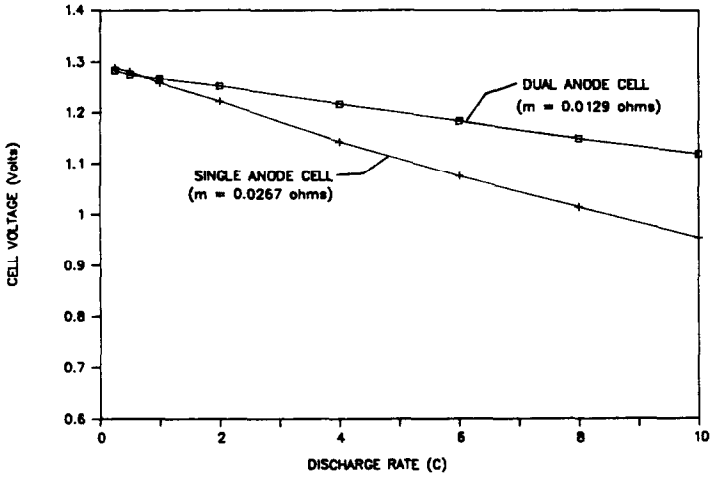

Fig. 6. Plot of mid-discharge cell voltages as a function of discharge rate to compare polarizations of the dual anode and single anode cell designs. $C = 1.3$.

of the discharge and at 75% DOD. At 50% DOD the difference between the dual anode cell and single anode cell was 10 mV at the C rate and 160 mV at the 10C rate. At 75% DOD the dual anode cell C rate voltage was still about 10 mV higher but at 10C the difference between the two increased to 230 mV. These data indicate the dual anode cell has a higher voltage throughout the discharge and has less polarization at the deeper depths-of-discharge than does the single anode cell. The slopes of the mid-discharge voltage curves were 12.9 mΩ for the dual anode and 26.7 mΩ for the single anode cell. The slopes of the curves in Fig. 7 were 20.1 mΩ for the dual

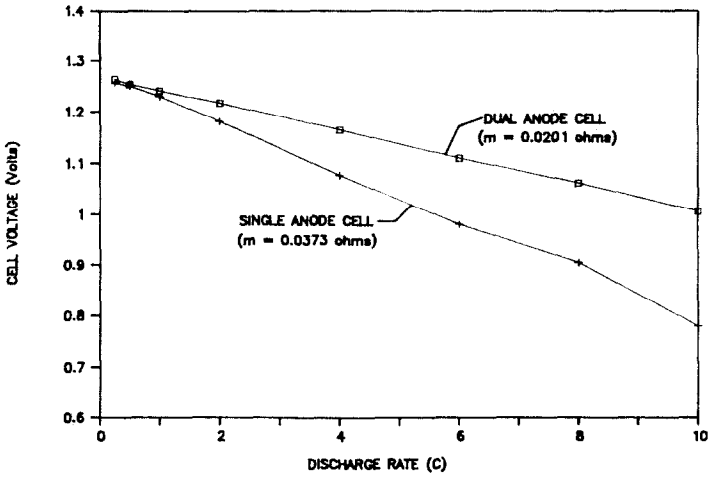

Fig. 7. Plot of cell voltages at 75% DOD as a function of discharge rate to compare polarizations of the dual anode and single anode cell designs. $C = 1.3$.

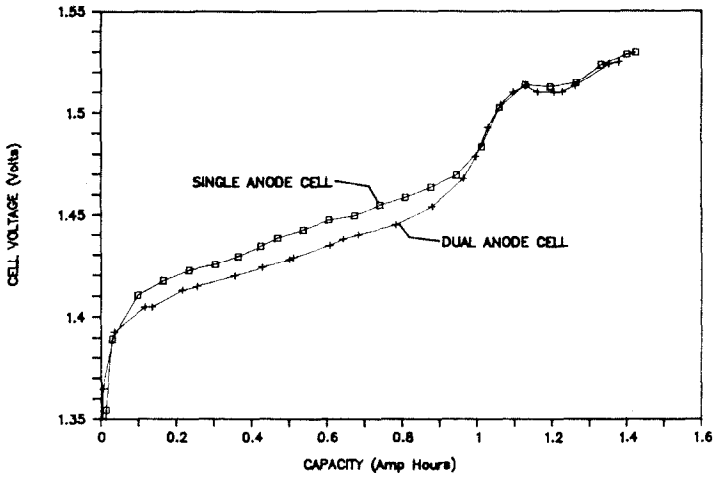

Fig. 8. Charge performance comparison at the $C/2$ rate. 10% overcharge, C discharge, $C/4$ drain. $C = 1.3$.

anode and 37.3 mΩ for the single anode cell. For both Figures the dual anode cell resistance is about one-half of the conventional cell resistance which is what was anticipated. The change in slope of the single anode cell resistance between 50% DOD and 75% DOD was 10.6 mΩ (37.3–26.7), whereas the dual anode cell only charged 7.2 mΩ (20.1–12.9).

A comparison of the charge performance at the $C/2$ rate is shown in Fig. 8. Up to approximately 75% state-of-charge (SOC) the dual anode voltage was 15 to 20 mV lower than the single anode cell. The rapid rise in the voltage is probably associated with the production of oxygen which was

consistent for both designs. The $C/2$ charge was used as the standard charge rate for the evaluation of the discharge performance. No other charge rates have been investigated.

Another objective of this study was to evaluate the dual anode cell design for pulse power applications. A comparison of the performance of both designs during an $8C$ standard constant current discharge and an $8C$ pulse discharge is shown in Fig. 9. During the pulse test the cell was alternately discharged at $8C$ (10.4 A) for 5 s then switched to open-circuit for 10 s until the cell voltage reached 0.1 V. The discharge voltage was taken at the end of the 5 s discharge period. The standard discharge was a continuous 10.4 A current until the cell voltage reached 0.1 V. The pulse discharge voltage for the dual anode cell was only about 10 mV higher than the voltage obtained during the constant current discharge. However, the pulse discharge voltage for the dual anode cell was about 120 mV higher than the pulse voltage for the single anode cell indicating a significant decrease in polarization effects with the dual anode design. This Figure also shows the pulse discharge voltage of the single anode cell is about 30 mV higher than the constant current discharge voltage. Comparison of the voltage difference between the standard and pulse discharges for both designs demonstrates the significant reduction in polarization in the cell when the second anode is used.

Both designs were also evaluated on pulse discharge at the $2C$ and $4C$ rates. Voltage curves were in the same order as the $8C$ discharges but the differences were less. A comparison of the pulse discharge voltage performance at $2C$ and $4C$ for the dual anode cell are compared with the $8C$ performance in Fig. 10. The improvement in performance of the dual anode cell over the conventional cell is shown in Fig. 11. Mid-point voltages for the pulse discharges are plotted against the discharge rate. At $2C$, $4C$ and $8C$ rates,

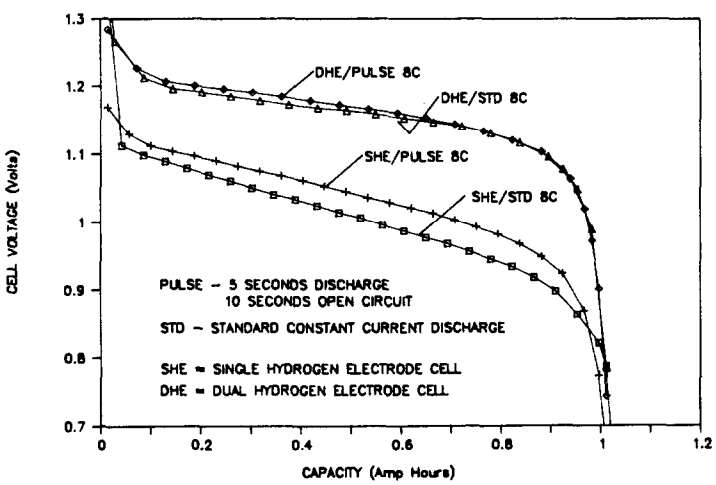

Fig. 9. Comparison of the $8C$ pulse discharge and $8C$ constant current discharge voltages. Pulse = 5 s discharge, 10 s open circuit. $C = 1.3$.

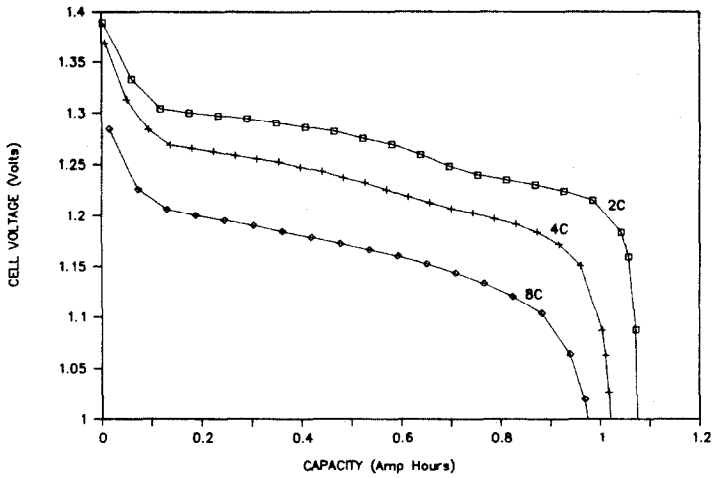

Fig. 10. Pulsed-current discharge voltage profile of the dual anode nickel–hydrogen cell. Voltage measured at base of electrodes. $C = 1.3$.

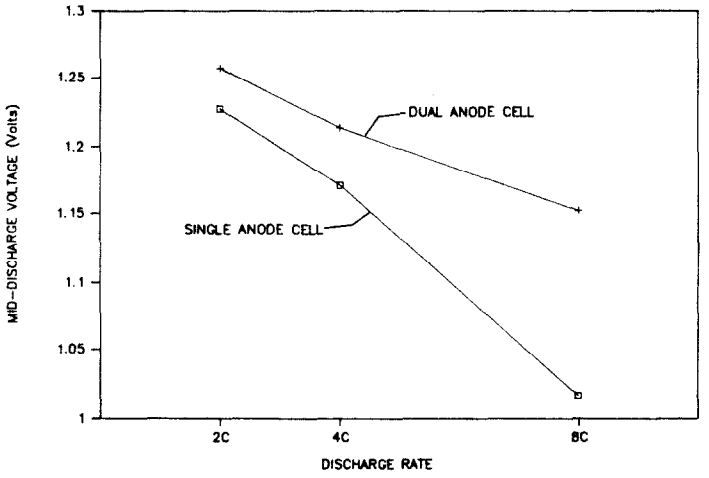

Fig. 11. Comparison of mid-discharge voltages of the single anode and dual anode cells during pulse discharges at $2C$, $4C$ and $8C$. $C = 1.3$.

the mid-discharge voltages of the dual anode cell were about 30, 40 and 140 mV, respectively, higher than the single anode cell.

The last test which was used to characterize the performance of the dual anode design was to make short duration charges and discharges at increasing currents while keeping the cell at approximately 50% SOC. After charging to 50% SOC the cell was charged at the first current for 15 s, switched to open-circuit for 3 min, 45 s, and then discharged at the same current for 15 s followed by another open circuit period. A comparison of the 15 s charge and discharge voltage performance is shown in Fig. 12.

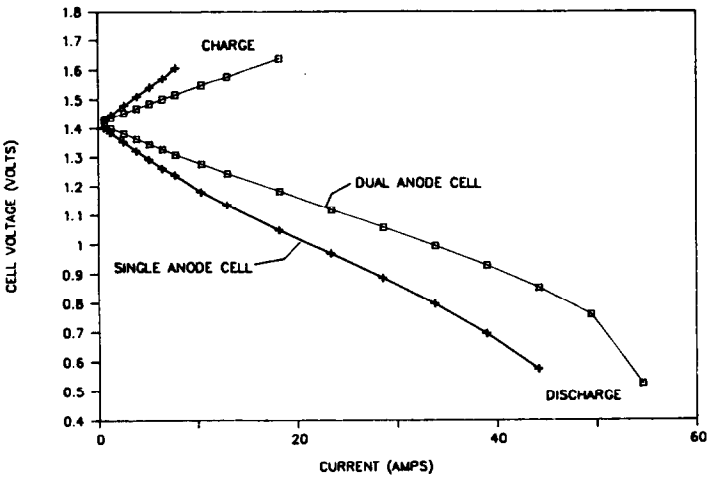

Fig. 12. Charge and discharge polarization measurements at 50% SOC. 15 s charge or discharge. Voltage measured at base of electrodes.

The charge characterization test was terminated after the voltage reached 1.6 V. In order to maintain the 50% SOC condition for the higher current discharges, the cell was charged at the *C* rate for the time necessary for each succeeding discharge.

The single anode cell reached 1.6 V on charge at 8 A whereas the dual anode cell did not reach 1.6 V until the charging current was 15 A. During the discharge test the single anode cell voltage dropped to 1.0 V at 21 A, however, the dual anode cell voltage did not reach 1.0 V until the current was about 33 A. This test, although not tied to any particular application, demonstrates the improved voltage performance on both charge and discharge for the dual anode cell design.

Summaries of the discharge power obtained from the two cell designs on the constant current and 15 s discharge tests are shown in Figs. 13 and 14. Figure 13 compares the power from the cell at the mid-points of the constant current discharges. The power outputs, plotted as a function of the discharge current, of the two designs are about the same below the 2*C* discharge rate (2.6 A) but gradually separate as the discharge current increases. At 13.0 A (10*C*) the power of the dual anode cell is 18% (15.0 versus 12.7 W) higher than the single anode cell.

A comparison of the power output as a function of the current of the two cell designs during the 15 s discharge test is shown in Fig. 14. The single anode cell reached a maximum power of 27 W at about 37 A. The dual anode cell's maximum power was 37 W at about 45 A which is a 37% higher power than the single anode cell. (Since the voltage measurements on these single nickel–hydrogen cells were taken at the base of the electrodes to eliminate voltage losses in the current collectors, these power values

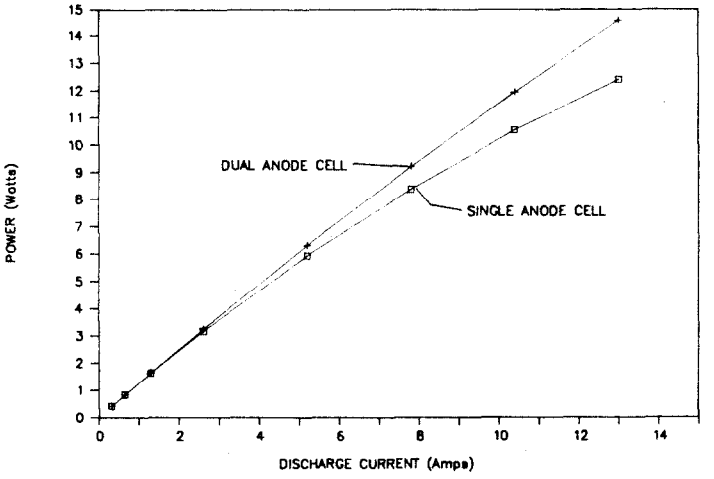

Fig. 13. Comparison of power outputs at 50% DOD during constant current discharges. $C = 1.3$.

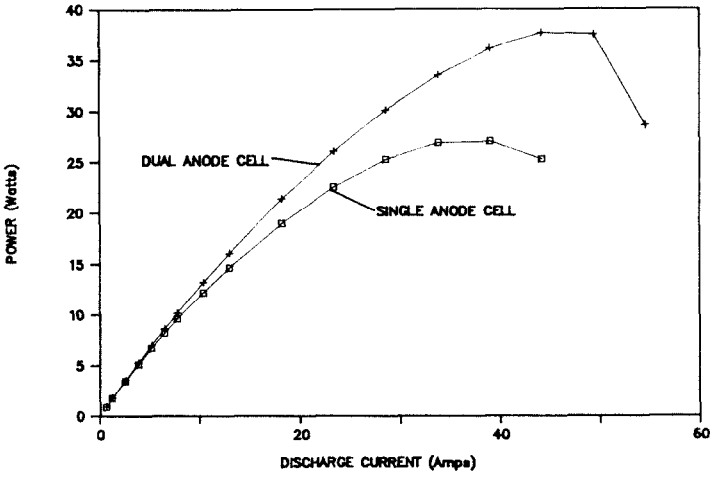

Fig. 14. Comparison of power outputs during discharge polarization test at 50% SOC. $C = 1.3$.

should not be used to project performances of higher capacity cells containing multiple cells.)

The results reported in this study were obtained using the same nickel electrode. The experiments were repeated twice and the results were in agreement. Other types of nickel electrodes and large nickel–hydrogen cell stack sizes need to be evaluated in order to assess the applicability of the dual anode concept.

Conclusions

The voltage performance of a single IPV nickel–hydrogen cell constructed with a hydrogen electrode on both sides of the nickel electrode was determined

and compared to a cell with the conventional design using a single hydrogen electrode. The same nickel electrode was tested in both cell designs. Constant current discharge voltages were compared from $C/4$ to $10C$ and five seconds pulse discharges were compared at $2C$, $4C$ and $8C$. Constant current charge performance was compared at the $C/2$ rate only. Fifteen seconds charges and discharges at 50% SOC were used to characterize the cells over a large range of currents and to determine the maximum discharge power of each cell.

In each test the dual anode cell voltage was higher on discharge and lower on charge than the single anode cell. Voltage anomalies at low currents ($C/4$, $C/2$) need to be clarified. Further studies with other nickel electrodes and multicell stacks are warranted to determine if the reduction in cell polarizations with the dual anode design justifies the additional component weight.

Acknowledgements

The author would like to acknowledge the assistance of Timothy Ryan and Michael Degen with the experimental work and data reduction for this study.

References

1 L. Miller, *Proc. 23rd IECEC*, Vol. 2, AMSE, New York, 1988, pp. 489–492.
2 H. S. Lim and S. A. Verzwyvelt, *J. Power Sources, 29* (1990) 503–519.
3 J. J. Smithrick and S. W. Hall, *Proc. 25th IECEC*, Vol. 3, AIChE, New York, 1990, pp. 16–21.
4 D. L. Britton, *Proc. 34th Int. Power Sources Symp.*, IEEE, NJ, 1990, pp. 235–238.
5 M. A. Reid, *J. Power Sources, 29* (1990) 467–476.